KTH Engineering Sciences

Application of Vortex Generators to a blunt body.

Technical Report

Torbjörn Gustavsson & Tomas Melin

Stockholm 2006

Preface

The work of this project was initiated by the idea of using aeroplane aerodynamics applied to drag reduction of land based vehicles.

The investigation has so far resulted in a literature study conducted by Torbjörn Gustavsson, a series of computer simulations and a series of wind-tunnel test. The result of the literature study is accounted for in "Alternative approaches to rear end drag reduction" and the result of the computer simulations and wind-tunnel test are presented in this report.

Torbjörn Gustavsson, M. Sc.
Web: www.vortaflow.com
E-mail: torbjorn@vortaflow.com

Tomas Melin, M Sc.
Web: www.flyg.kth.se
E-mail: melin@kth.se

Abstract

As an introduction the report will briefly mention something about the need of drag reduction of commercial vehicles.

The main focus of the report is on the work carried out during autumn of 2003 and spring 2004 reporting the results of computer simulations done on KTH and wind-tunnel tests performed at Västerås wind-tunnel facility.

Table of contents

1 Nomenclature and abbrevations

2D	two-dimensional
α	boat-tail angle
β	angle of inclination for VGs against the airflow
δ	boundary layer thickness
ρ	air density = 1.225 [kg/m^3]
μ	absolute viscosity coefficient = $1.7894 \times 10^{-5} \left[\dfrac{kg}{m \cdot s}\right]$ at standard sea-level
ΔC_{pmin}	difference in minimal pressure
C_d	drag coefficient
p	pressure
SNRA	Swedish National Road Administration
U	air speed [m/s]
VG	vortex generator
x	distance

2 Introduction

Aerodynamic drag of a commercial vehicle is a large part of the vehicles fuel consumption, according to Hucho [1] it can contribute to as much as 60 % of the vehicles fuel consumption during specific driving conditions.

So far aerodynamic design of commercial vehicles has concentrated on the front end of the vehicle. Since the front produce most drag it has been the most urgent part to optimise. This optimisation can easily be spotted on trucks and tourist coaches today. The rear end configuration has up until recently been neglected but Gilhaus [2] acknowledge the fact that on tourist coaches the rear end can contribute to as much as 27 % of the over all drag.

General methods of reducing rear end drag is boat-tailing and round rear edges and those are so far the methods considered most efficient. The difficulty using boat-tailing is that it reduces room for passengers and load significantly if major reductions in drag is to be expected. Rounded rear edges contribute to some reduced drag and aren't affecting the loading capability in the same way.

It would be beneficial to find a way past these problems and find a method for reducing rear end drag that don't affect the interior space of a vehicle too much.

Hucho [1] mentions an alternative approach to reducing base drag on blunt vehicles called "energizing the dead water". The basic principal is described in figure 1 b and is based on that the airflow from the sides (or in this case underneath) of the vehicle is in one way or another forced into baseflow of the vehicle - the area behind a blunt body with separated airflow. This is to increase the base pressure and thus reduce aerodynamic drag on the vehicle. None of the technologies described [1] generate enough basedrag reduction to be beneficial to use in the search for increased fuel performance.
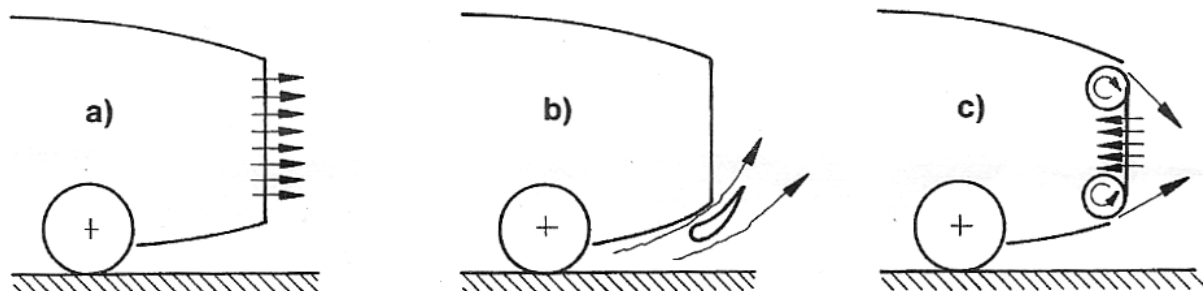
Figure 1 (a-c): Different technologies to reduce drag: a) Base bleed; b) Energizing the dead water; c) Reduction of effective base area. [1]

W. Calarese et. al. [3] achieved beneficial drag reduction when applying low-profile vortex generators (VGs) circumferentially around the fuselage of a C-130 aircraft body. Vortex generators have normally been used to increase low speed, high angle performance on aircraft wings and to reattach separated flow on airfoils. On a flap deflection of 35° Lin et. al. [4] managed to reattach the airflow completely where the airflow normally separates at approximately 12°. This is one of the reasons to why the authors of this paper wanted to try this approach on ground vehicles.

3 Vortex Generators on road vehicles

Vortex generators on road vehicles has been suggested by S. O. Ridder [5] but then only in limited use on the roof of a hatchback to reattach the flow and thus reduce soiling of the rear window. Due to limitations set up by Swedish National Road Administration (SNRA, Vägverket) it is not allowed to have any parts of the vehicle extend outside of the vehicle perimeters. Therefore an alternative approach was chosen where the VGs are placed just behind the shoulder of the body as explained in figure 2 a and b.

a) Vortex generators diverting airflow when in use on a passenger car, side view
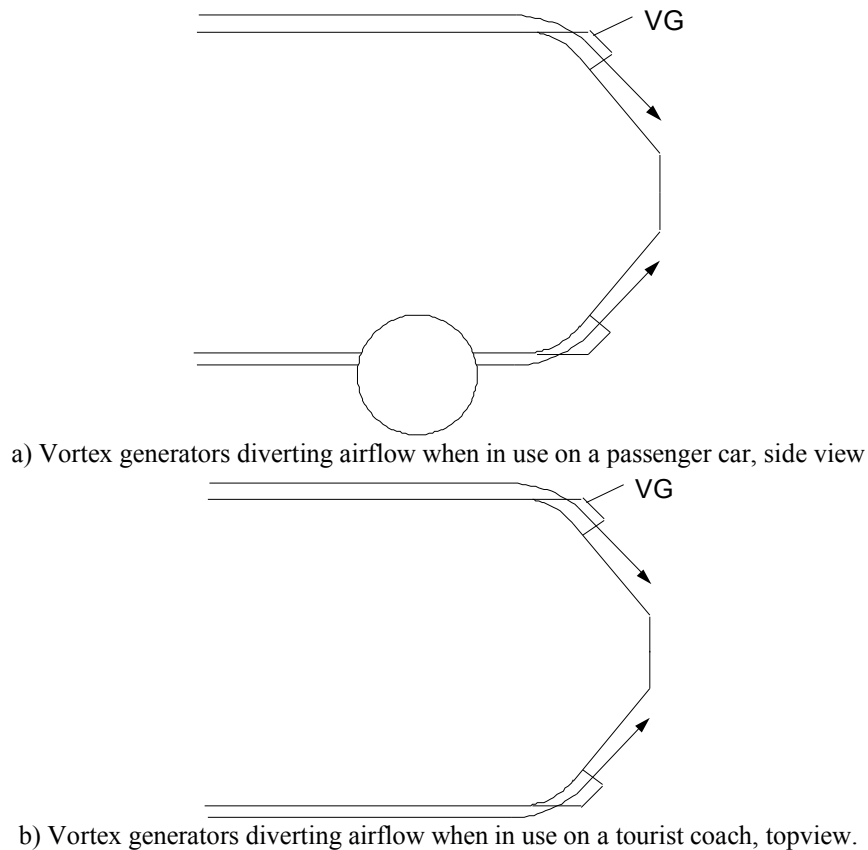
b) Vortex generators diverting airflow when in use on a tourist coach, topview.
Figure 2 (a-b): The idea of use of vortex generators due to limitation of SNRA.

The purpose is the same as when using the method of "energizing the dead water" – increased pressure over the rear end on a blunt body to reduce pressure drag and thus reduce aerodynamic drag. The author has performed a series of tests with this strategy in mind and initial simulations were done in Xfoil and some wind-tunnel tests were performed at Mälardalens University.

4 Xfoil simulations

Simulations were done using Xfoil [6] software to simulate a blunt body with a boat tail. Xfoil is "an interactive program for the design and analysis of subsonic isolated airfoils" [6].

Extreme streamlining of the front end was necessary to make the calculations converge in Xfoil. Different α angles of boat tailing was evaluated but the program did not converge for α larger than 34° due to problems of simulating turbulent flow since the software only can handle "limited trailing edge separation" [6]. Simulations were made with variation of rear edge radius as defined by figure 3 and table 1.
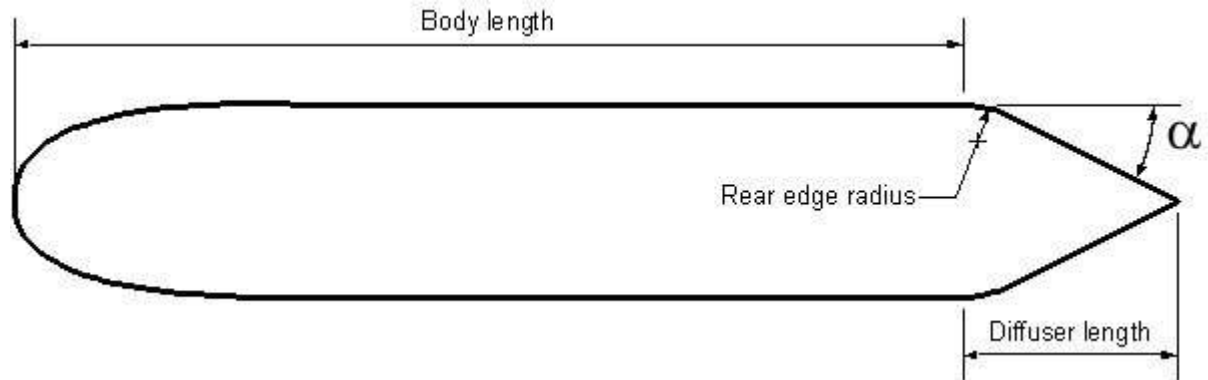
Figure 3: Definitions of measurements of body simulated in Xfoil.

The bodys overall length is 12 m from front to where the rear edge radius begin and its width is 2.55 m. Reynolds number of choice is $2.0 \cdot 10^6$ and angle of attack is $\theta = 0°$. The boat-tail length (= diffuser length) is approximately given by equation 1.

$$L_{tail} = \frac{2.55}{2} \cdot \arccos(\alpha)$$
(1)

Rear edge radius [m]	α = 20° C_d	α = 30° C_d
0.1	0.17309	Nan
0.3	0.17342	0.55140
0.5	0.17210	0.47957
0.7	NaN	0.47331
0.9	0.16702	0.41969
1.1	0.16626	0.37941
1.3	0.16559	0.37676
1.5	0.16471	0.37272
1.7	0.16353	0.34996
1.9	0.16034	0.32647
2.1	0.15910	0.32014
2.5	0.15696	0.31185
3	0.15476	Nan
3.5	0.15266	0.26975
4	0.15050	0.25913

Table 1: Variations of variables during bluff body simulations in Xfoil.

4.1 Presentation of Xfoil results

According to Hucho [1] and R H Barnard [7] 20° should be the "best case scenario" and 30° the "worst case scenario" (= Karmann body) or at least very close to those cases. For those reasons an α angle of 20° and 30° were the angles of choice when simulations were made.

The body coordinates are defined by Matlab code written in cooperation with Tomas Melin and is accounted for at [8].

Figure 4 a-c illustrate pressure distribution for different cases of rear-end radius when boat-tail angle is 20°.
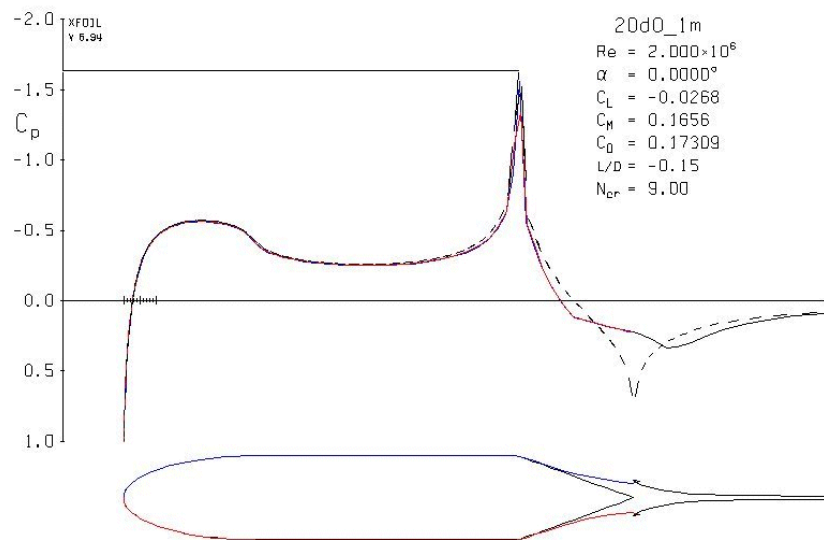
a) Rear edge radius = 0.1 m

b) Rear edge radius = 1.7 m
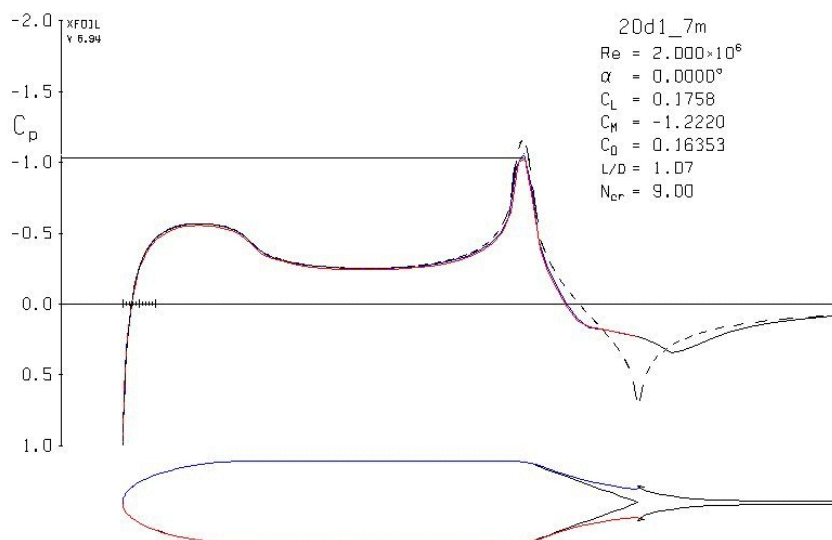
c) Rear edge radius = 4 m
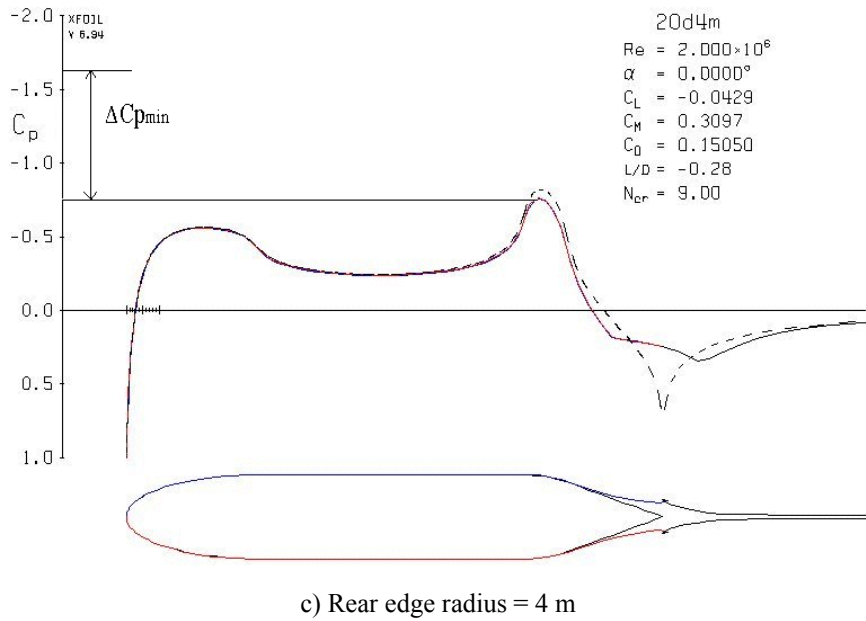
Figure 4 (a-c): Simulations of a blunt body in Xfoil with a 20° boat-tail.

As can be seen in figure 4 a-c there is a pressure drop at the front end of the body. This is can be explained using the Bernoulli equation defined in equation 2 [9].

$$p + \frac{1}{2} \cdot \rho \cdot U^2 = const \qquad (2)$$

Airspeed is increased around the front end of the vehicle and thus the pressure decrease. The same thing happen at the rear end when the body is tapered into the boat-tail. The body in figure 4 a has lower radius on the rear end corner and then demonstrate a more violent pressure drop than the other cases in figures 4 b and c. This pressure drop in figure 4 a indicate that the flow is more lightly to separate at this point and the pressure drop in it self create pressure drag that explain the increase in drag for the cases when rear edge radius is low. This difference is illustrated by ΔC_{pmin} in figure 4c. The same behaviour can be seen in figure 5 a-c where the boat-tail angle is 30°.

a) Rear edge radius = 0.3 m
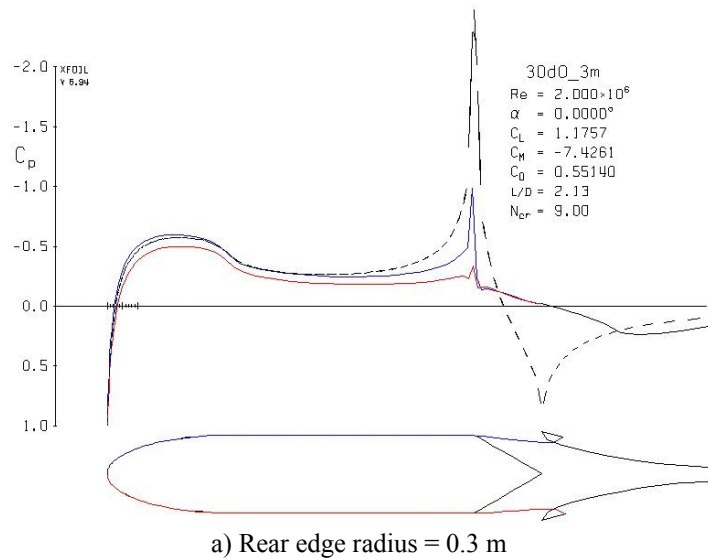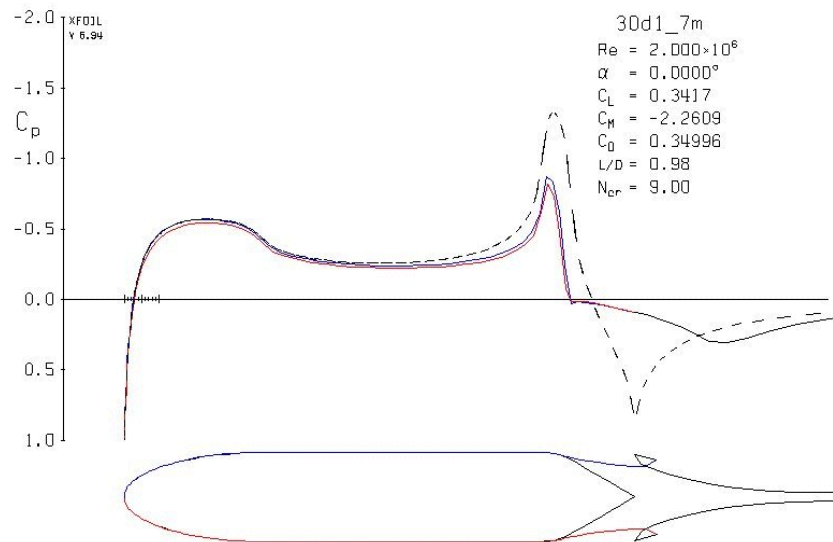
b) Rear edge radius = 1.7 m
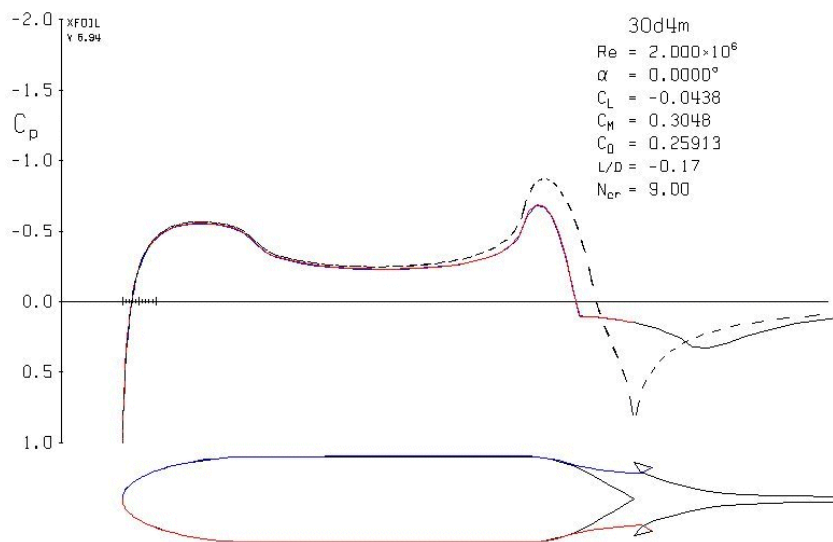
c) Rear edge radius = 4 m

Figure 5 (a-c): Simulations of a blunt body in Xfoil with a 30° boat-tail.

In the case of 30° boat-tail the body is more sensitive to change in rear end radius. For the case when the radius is 0.3 m (figure 5 a) the flow separates completely at the rear end edge and course a pressure drag that result in a C_d of 0.55 compared to the C_d of 0.25 for a 4 m rear edge radius (figure 5 c) where the flow is attached longer and the pressure drop isn't that violent. Cd for the different configurations are compared in figure 6.
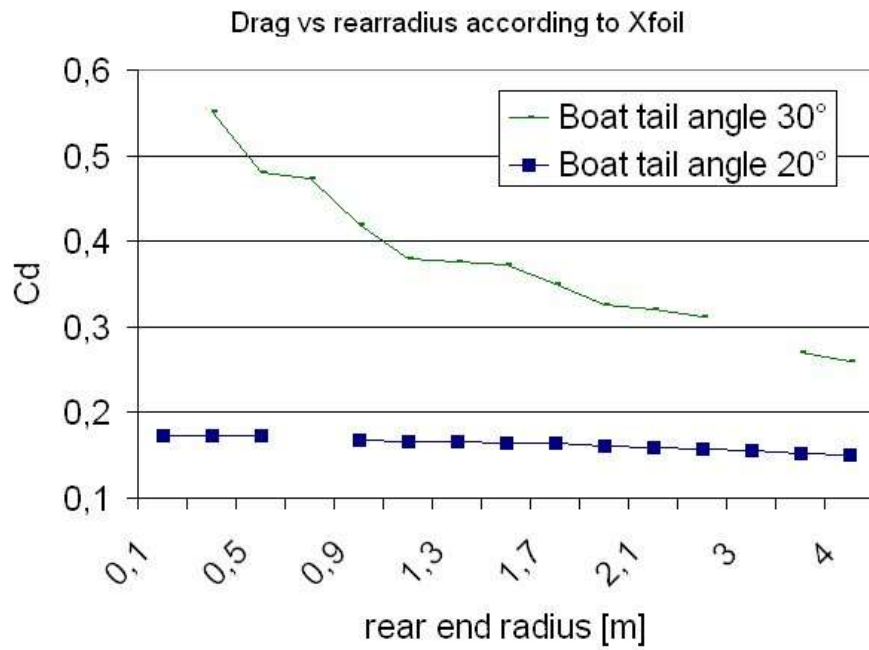
Figure 6: Comparison of different Cd for different rear end radius in the cases of 20° and 30° boat-tail as simulated by Xfoil.

As expected from Hucho [1] and Barnard [7] the drag for the body with 20° boat-tail is much lower than the case for a 30° boat-tail.

5 Wind-tunnel tests

A series of wind-tunnel tests were performed at Mälardalen University closed circuit wind-tunnel in Västerås.

5.1 Wind-tunnel definitions

The Västerås wind tunnel is a closed circuit wind tunnel that is generally described by figure 7 where the flow is clock-wise.
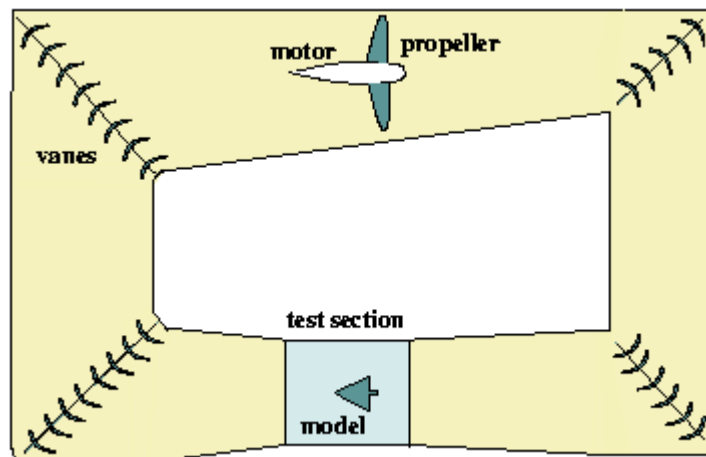
Figure 7: General description of a closed circuit wind-tunnel. [10]

A detailed description of the Västerås wind-tunnel facility is given in appendix 1.

5.1.1 Wind-tunnel balance

In the test section of the tunnel there was a balance mounted generally described by figure 8, a detailed description of it can be found in appendix 2. The loading cell is mounted between the two top plates. The model is bolted onto the top of the table and can move back and forth and thus register the amount of force actuated on it. A picture of when a model is mounted onto the balance when it is place in the test section can be found in figure 13.

Figure 8: General description of the wind-tunnel balance used at tests in Västerås. The loading cell that measure the aerodynamic drag is mounted between the two plates at the top of the balance and the model is rigidly mounted on the top plate.

5.2 Primary wind tunnel tests

The aim of the tests was to evaluate the possibility to use of VGs placed behind the shoulder of an extreme boat-tail as described in figure 2. Initial tests were performed 2003-09-11 and the goal of these tests was to confirm that the airflow was redirected as indicated in figure 2. A large body generally described in figure 9 a-c with smooth front end was placed in the test section to show that it was possible to redirect the flow as predicted.

a) Topview

b) Side view

c) Slightly from behind

Figure 9 (a-c): The general shape of the body used to show it is possible to redirect airflow with the use of VGs just behind the shoulder of a boat-tail. Length: 95 cm, width: 50 cm and height: 30 cm.

The tests were successful, the airflow was redirected as figure 2 indicates which figure 10 show. When the VGs are removed the airflow is clearly separated as figure 11 show.

Figure 10: The airflow over a general body is redirected over the sharp 40° boat-tail using VGs to redirect the flow.

Figure 11: The airflow clearly separates when VGs are removed from the 40° boat-tail.

5.3 *Secondary wind tunnel tests*

The tests at 2003-09-11 indicated that the technology worked as predicted but it still wasn't established that the drag of the body was reduced diverting the flow with VGs. For this another series of tests took place 2003-10-03. The purpose of them was to establish if and in that case how much drag cold be reduced using VGs mounted behind an boat-tail shoulder of more than 20°.

5.3.1 Channel for undisturbed flow

A channel described in figure 12 a-b was constructed to produce undisturbed 2D flow over a new body composed to evaluate drag reduction capability for VGs.
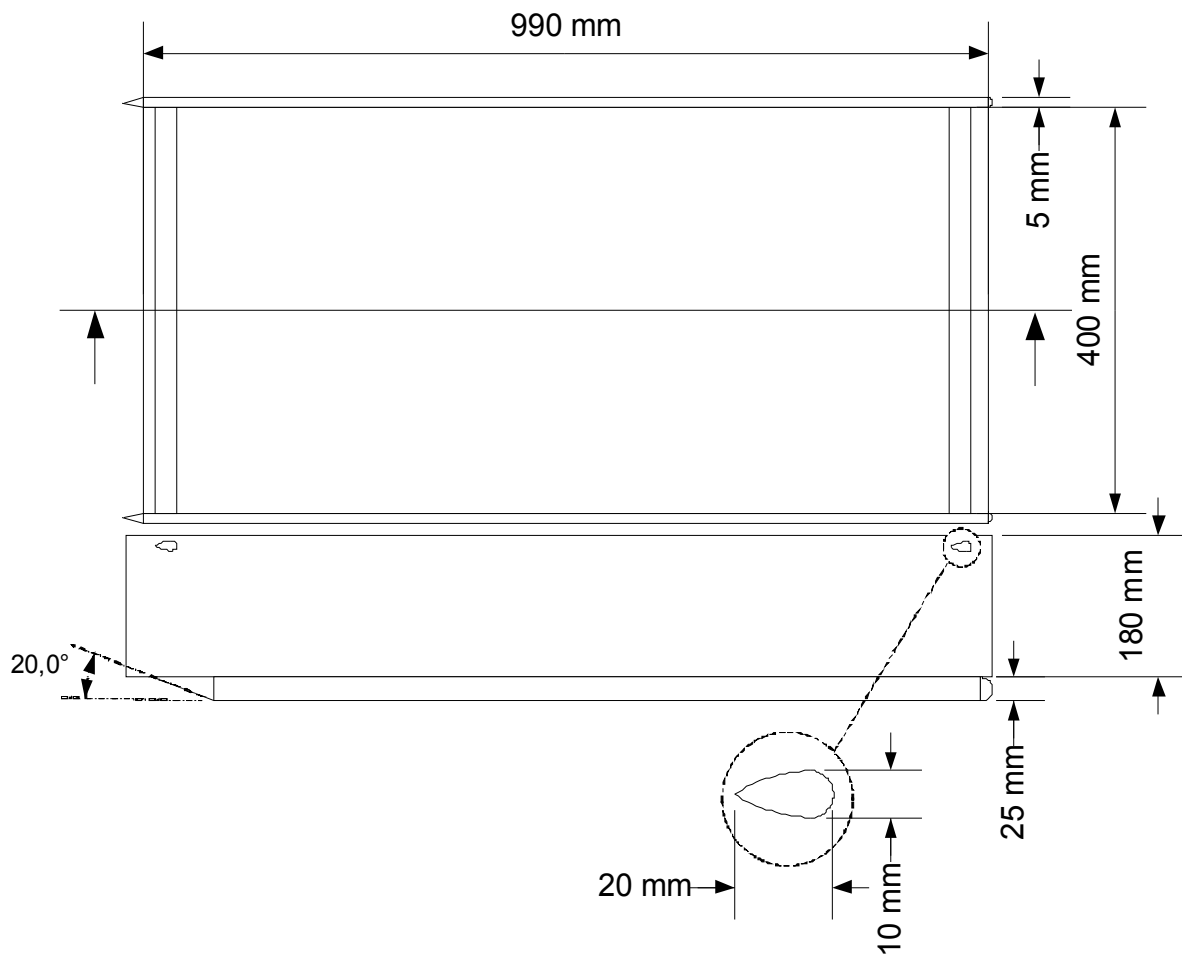
a) Top and side view of the channel
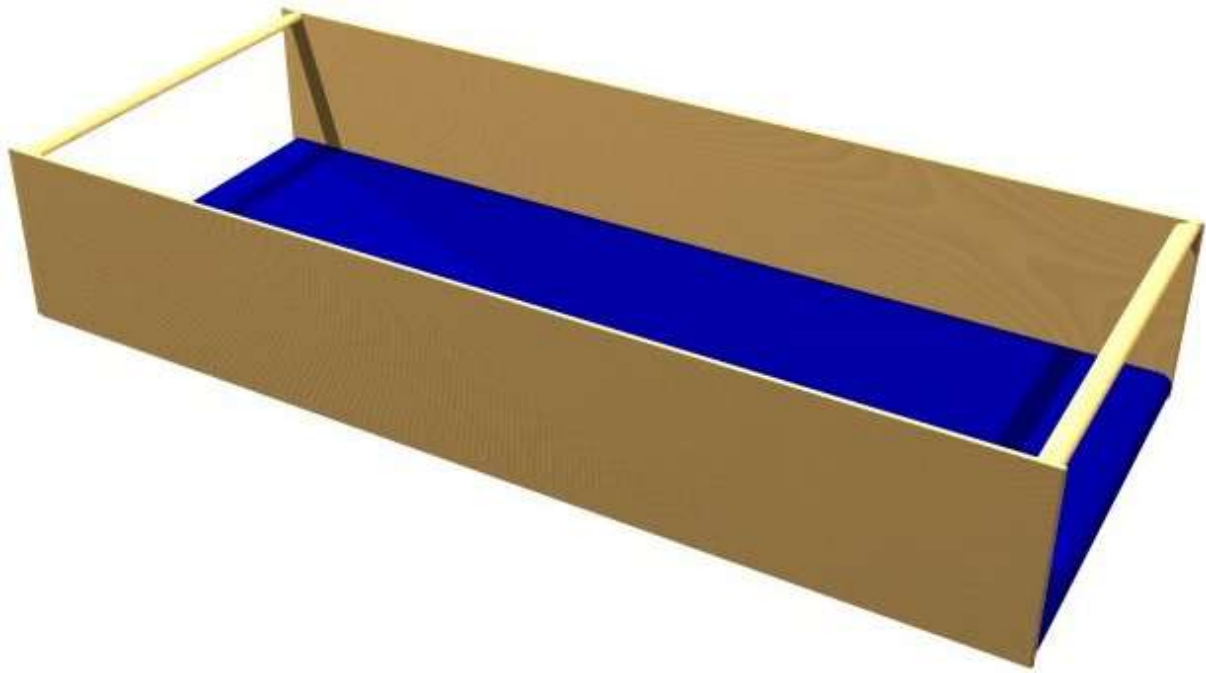
b) Overview of the channel
Figure 12 (a-b): Description of the channel made for producing 2D flow over a bluff body.

The geometry of the channel is based on two assumptions:
1) It must be long enough to generate turbulent flow.
2) Its walls must be high enough to keep the airflow strictly two-dimensional.

The transition from laminar to turbulent flow takes place when Reynolds number exceeds $5 \cdot 10^5$ where Reynolds number is defined by equation 3 [9]:

$$\mathrm{Re}_x = \frac{\rho \cdot U \cdot x}{\mu} \qquad (3)$$

If it is desirable to generate turbulent airflow after for example 0.5 m it is necessary to have airspeed of 14.6 m/s as shown by equation 4.

$$\mathrm{Re}_x = \frac{\rho \cdot U \cdot x}{\mu} \Rightarrow \frac{\mathrm{Re}_x \cdot \mu}{\rho \cdot x} = \frac{5 \cdot 10^5 \cdot 1.7894 \cdot 10^{-5}}{1.225 \cdot 0.5} = U = 14.6 \, \frac{m}{s} \qquad (4)$$

It is now known that in order to generate turbulent flow we need to exceed 15 m/s in airspeed in the wind-tunnel and that take care of assumption number 1. To make sure that the airflow is strictly two dimensional it is necessary to make sure that the walls of the channel is that high that the flow doesn't interact with flow outside of the channel.

In the definition of the wind-tunnel data it is stated that the maximum airspeed is 60 m/s and the channel is 0.99 m long according to figure 12. This gives us a Reynolds number of:

$$\mathrm{Re}_x = \frac{\rho \cdot U \cdot x}{\mu} = \frac{1.225 \cdot 60 \cdot 0.99}{1.7894 \cdot 10^{-5}} = 4.07 \cdot 10^6 \qquad (5)$$

According to Anderson [9] the definition of turbulent boundary layer thickness is:

$$\delta_{turbulent} = \frac{0.37 \cdot x}{Re_x^{0.2}} \qquad (6)$$

This gives a boundary layer thickness of:

$$\delta_{turbulent} = \frac{0.37 \cdot x}{Re_x^{0.2}} = \frac{0.37 \cdot 0.99}{(4.02 \cdot 10^6)^{0.2}} = 0,017\,\text{m} \qquad (7)$$

The channel walls height of 0.18 m is more than adequate for our needs even though the boat-tail body of height 0.09 m is mounted in the channel.

Skin friction coefficient is defined for a turbulent boundary layer as [9]:

$$C_{f,turbulent} = \frac{0.074}{Re_x^{0.2}} \qquad (8)$$

And that give:

$$C_{f,turbulent} = \frac{0.074}{Re_x^{0.2}} = \frac{0.074}{\left(4.07 \cdot 10^6\right)^{0.2}} = 0,0035 \qquad (9)$$

Drag for a flat plate is defined as [9]:

$$D_f = q_\infty \cdot C_f \cdot S \qquad (10)$$

where q_∞ is the dynamic pressure $= \frac{1}{2} \cdot \rho \cdot U^2$ and S is the overall surface area:

$$D_f = 0.5 \cdot 1.225 \cdot 60^2 \cdot 0.0035 \cdot \left(0.18 \cdot 1 \cdot 4 + 0.4 \cdot 1 \cdot 2\right) = 11.8\,\text{N} \qquad (11)$$

Compared to the results measured shown in figure 14 the estimated drag is much lower than the measured one. This is because of the manufacturing method of the channel. Due to lack of founding it was not possible to create a channel with perfect surfaces but there are several edges and additional drag generated by screws, joints and glue on several surfaces, on the outside of the channel not to effect the quality of the flow in the channel, that translates to larger drag than predicted by equation 7. That is why the drag of the empty channel was measured so it could be subtracted from the values received with a body as described later.

5.4 Wind-tunnel test results

The empty channel, described in figure 12, was rigidly mounted onto the balance, described by figure 8 and appendix 2. The balance and the channel were mounted into the test section of the wind-tunnel, as described by figure 13, to measure the drag of the empty channel as presented in figure 14.
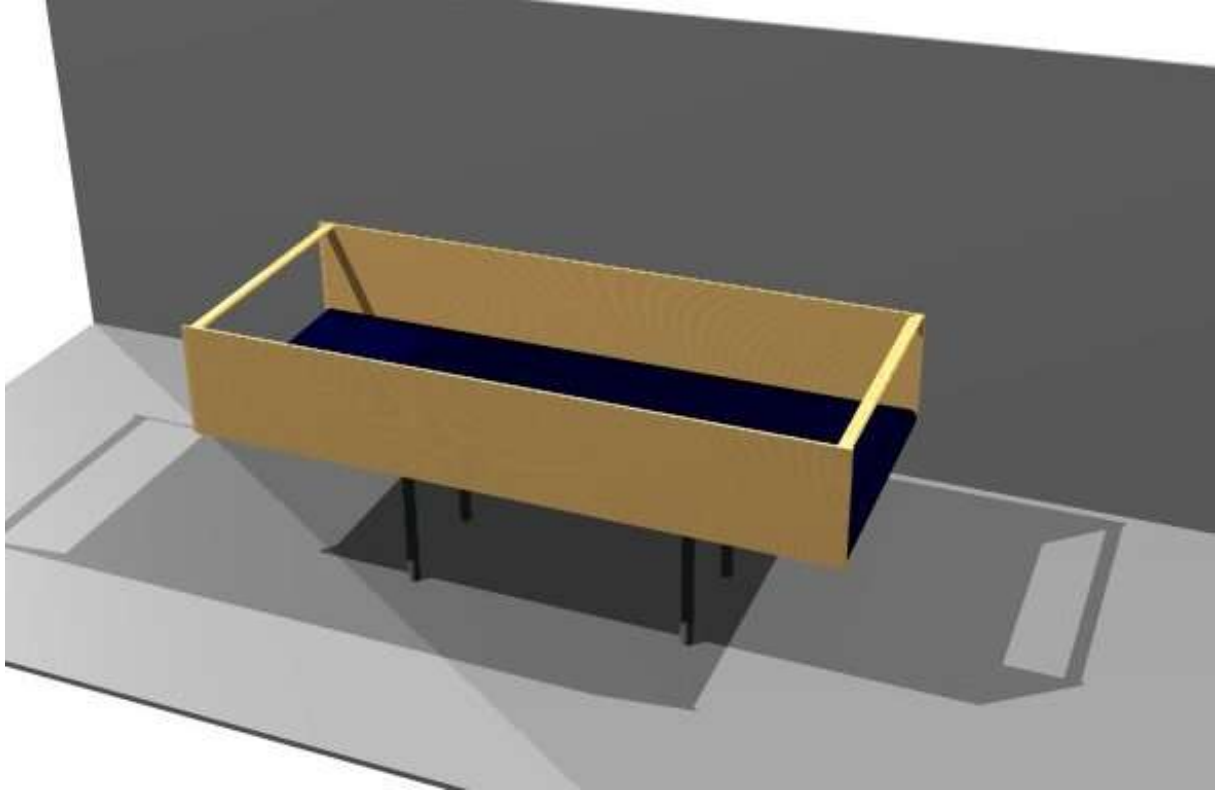
Figure 13: The empty channel was mounted onto the balance to measure its drag. Not shown are the fairings of the legs to the balance. These can be seen in figure 17.
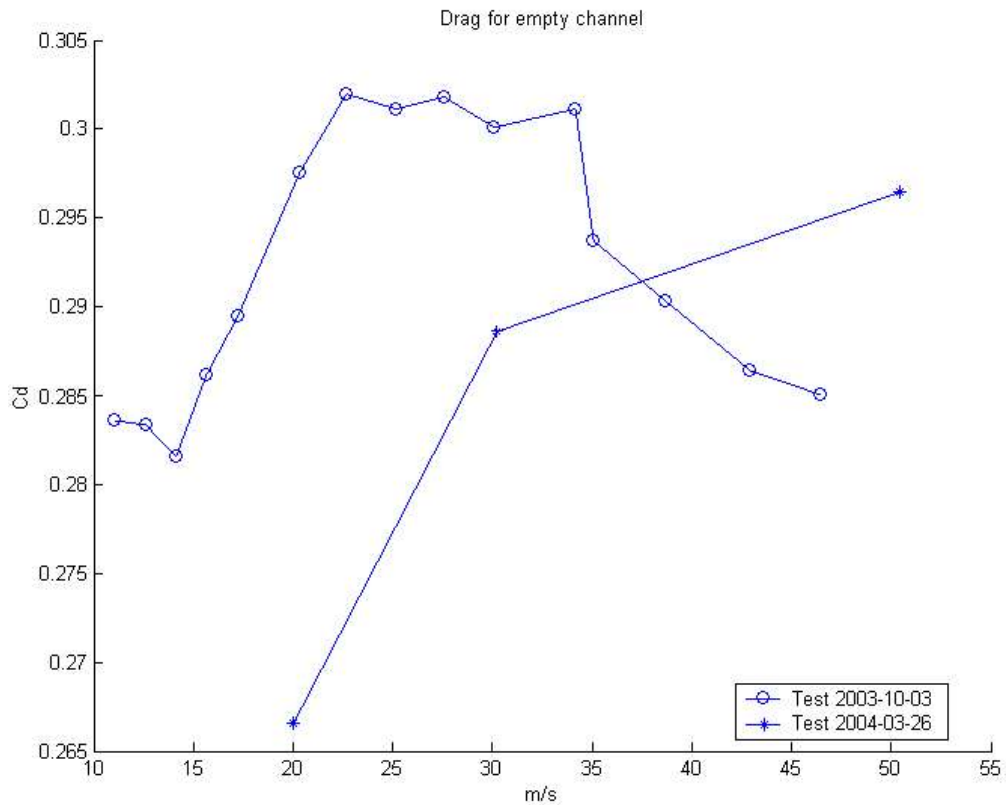
Figure 14: Drag of the empty channel.

The body mounted into the channel is described by figure 15 (a-d).
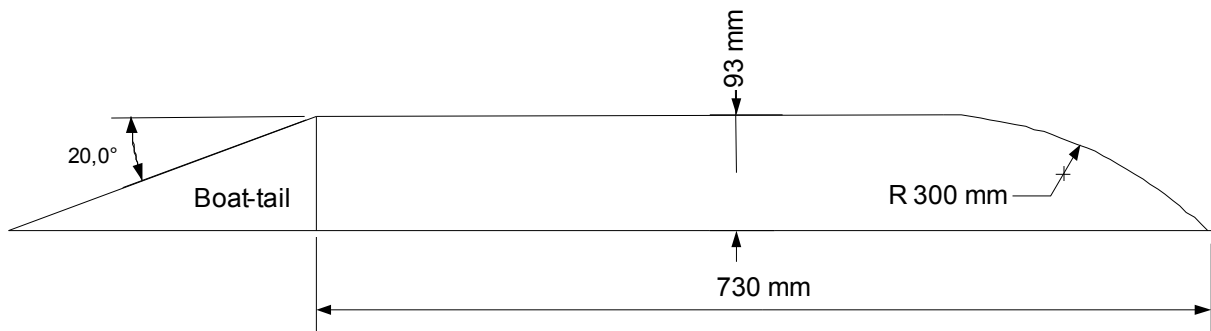
a) Dimensions of the body mounted in the channel where the centre of radius is located under the point where the flat part of the body begins. The part behind the 730 mm long forebody is called a boat-tail and is interchangeable with different tails as described by figure 15 d.
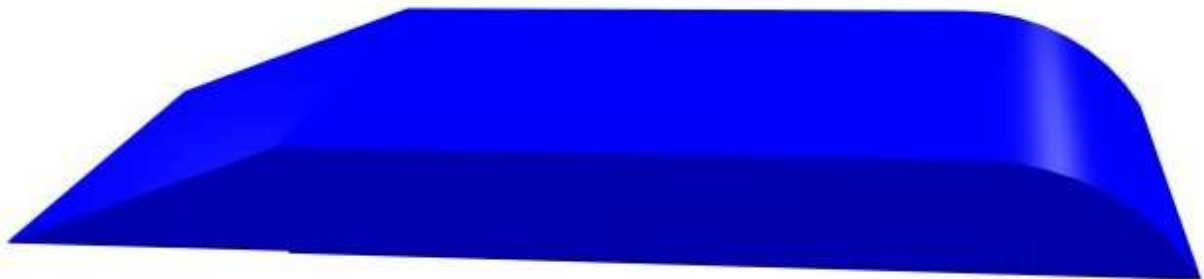
b) 20° boat-tail.
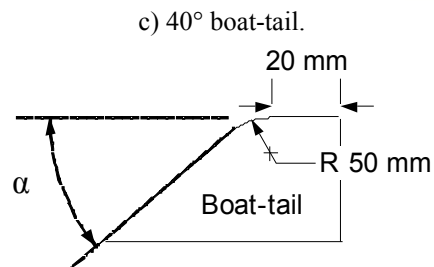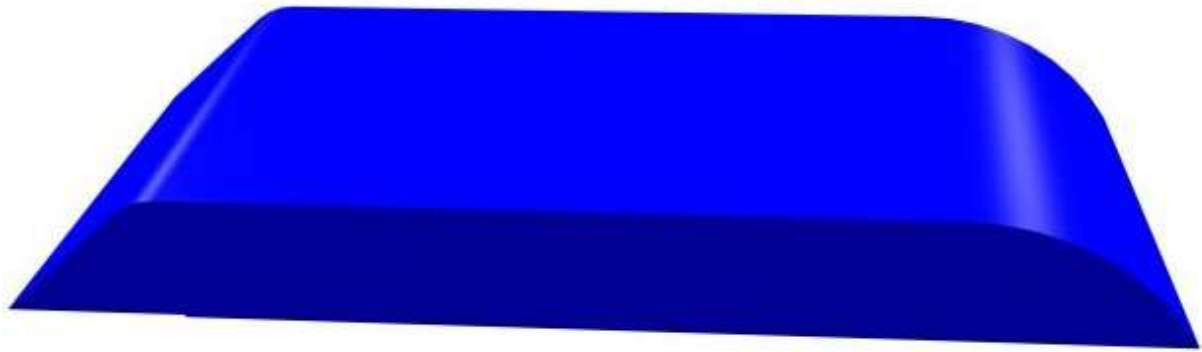
c) 40° boat-tail.

d) Boat-tail with α-angle over 20°. It varied according to table 2. On some tests there were VGs mounted and some there were no VGs mounted. To create a 90° boat-tail the boat-tail section was completely removed.
Figure 15 a-d: Body mounted into the channel to create different diffusers/ boat-tails. The bodies width is the full channel width of 40 cm.

Figure 15 d describe how the different boat-tails was constructed with varying angle α.

How the body was mounted into the channel is described by picture 16 a and b. In all the pictures the airflow comes from the right side.
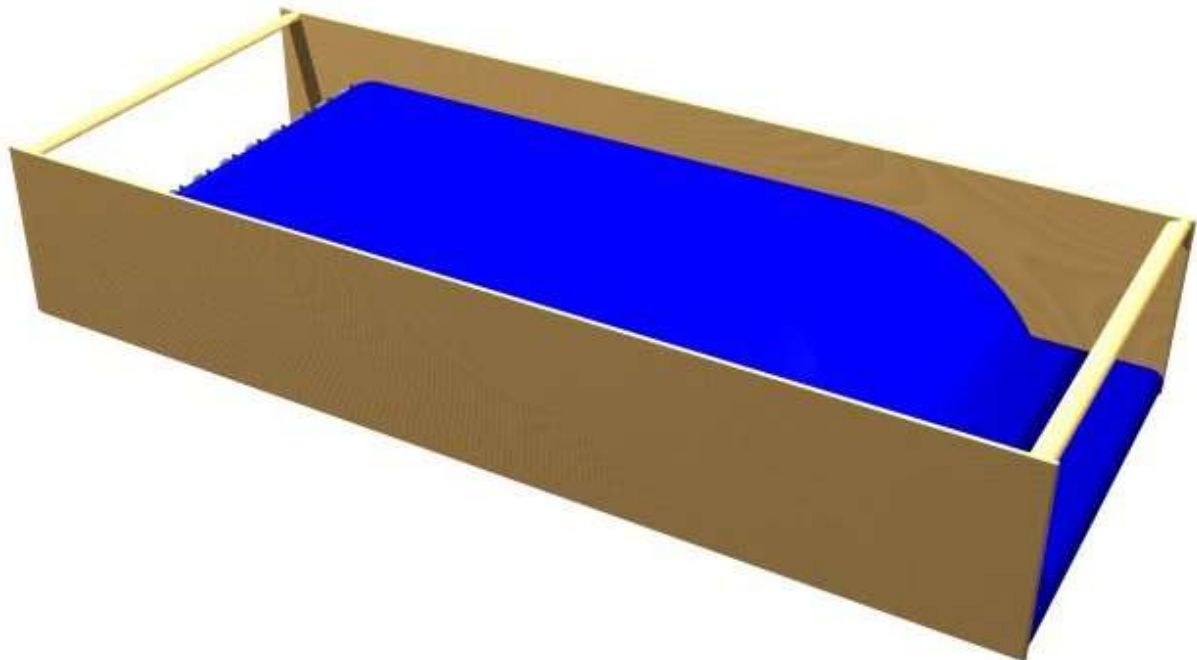
a) A 40° boat-tail body mounted into the channel with VGs placed just behind the shoulder.
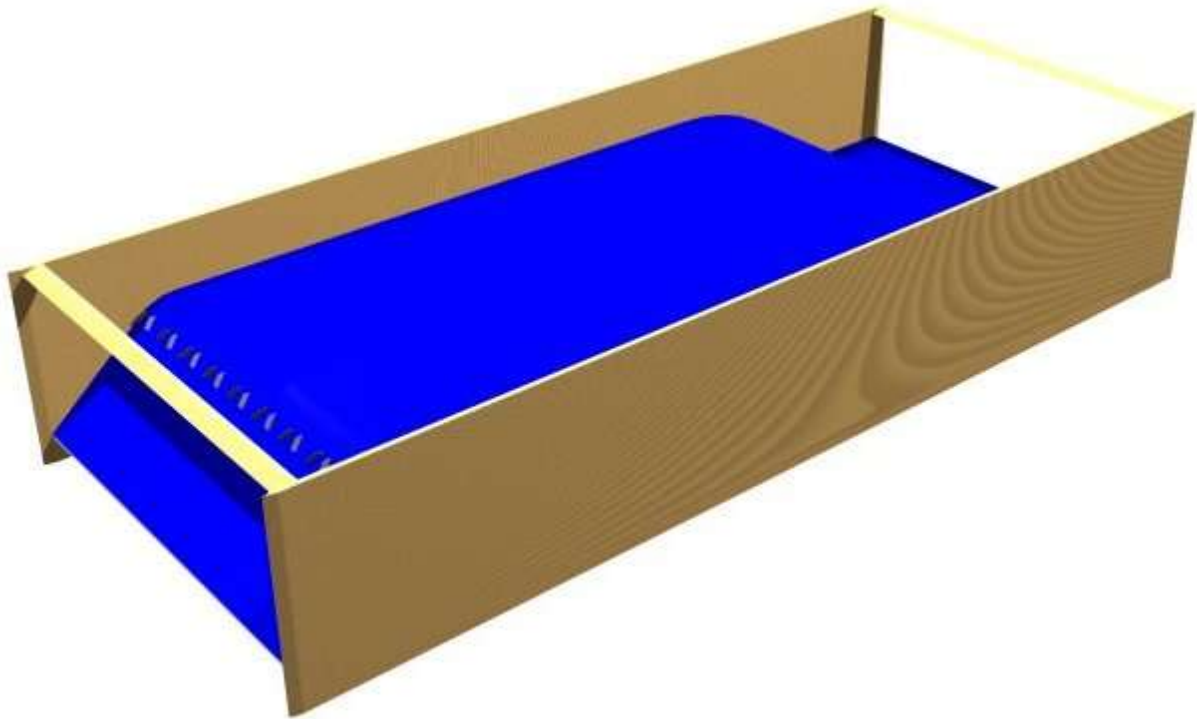
b) A 40° boat-tail body mounted into the channel with VGs placed just behind the shoulder.
Figure 16 (a-b): Different views of boat-tail body mounted into the channel earlier described.

Figure 17 show the body mounted in the channel when the channel is mounted on the balance in the wind-tunnel test section.
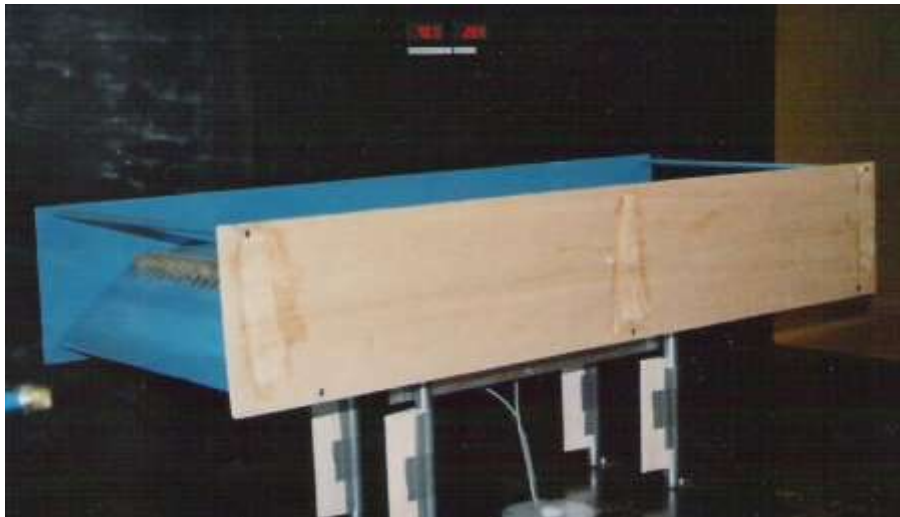
Figure 17: A photo of the channel with a 40° boat-tail body mounted on the balance in the tunnel. Fairings are mounted on the legs of the balance to reduce turbulence in the tunnel.

Different body configurations were tested by varying the diffuser/ boat-tail angle, VGs on/off, generating co- and counter-rotating vortices and different spacing between VGs as described by table 2.

Test	Degree on boat-tail	H [mm]	L [mm]	β [°]	co-/counter-rotating	Spacing [mm]
01	Empty channel					
02	90°					
03	20°					
04	40°	5	10	20	counter	13/18
05	40°	5	10	20	co	20
06	40°	5	10	20	co	40
07	40°					
08	40°	10	5	20	co	20
09	40°	10	5	20	co	40
10	40°					
11	40°	15	0	20	counter	20/30
12	40°	15	0	20	co	40
13	50°					
14	60°					
15	60°	5	15	20	co	20
16	60°	10	5	20	co	40
17	60°	15	10	20	co	40
18	20°					

Table 2: Different variables tested at Västerås wind-tunnel facility. In the case of VGs were mounted on the boattail this is indicated by the fact that their dimension are defined in the table.

As limitations by SNRA prescribe (figure 2 a and b) not any part of the VGs was extended outside of the body but mounted below the top line defined figure 18 a. The top line is the line that follows the top of the body mounted in the channel.
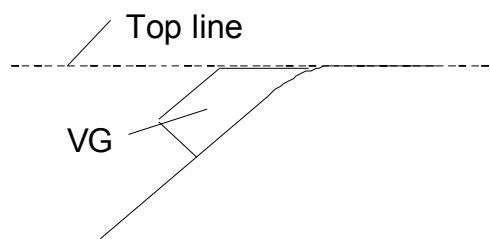
a) The VG was never mounted above the top line of the body defined in figure 15 a.
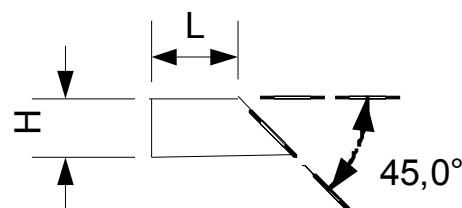
b) Definitions of measurements of VGs used in table 2
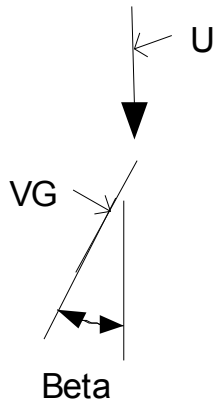
c) Definition of the inclination (angle β) of VG towards the freestream U.

Co-rotating VGs

Distance 3
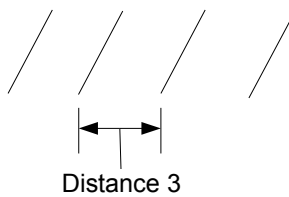
Counter-rotating VGs

Distance 2   Distance 1
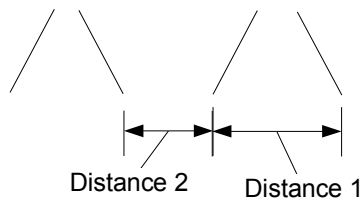
d) Difference in the mounting of VGs for generating co-rotating or counter-rotating vorticies.
Figure 18 (a-d): Definitions of different VG configurations.

Figures 19 and 20 show that the drag varies with different angels of boat-tailing as expected by the simulations made in Xfoil. The increase in C_d is probably from the fact that that the turbulent layer isn't fully developed before 23 m/s.
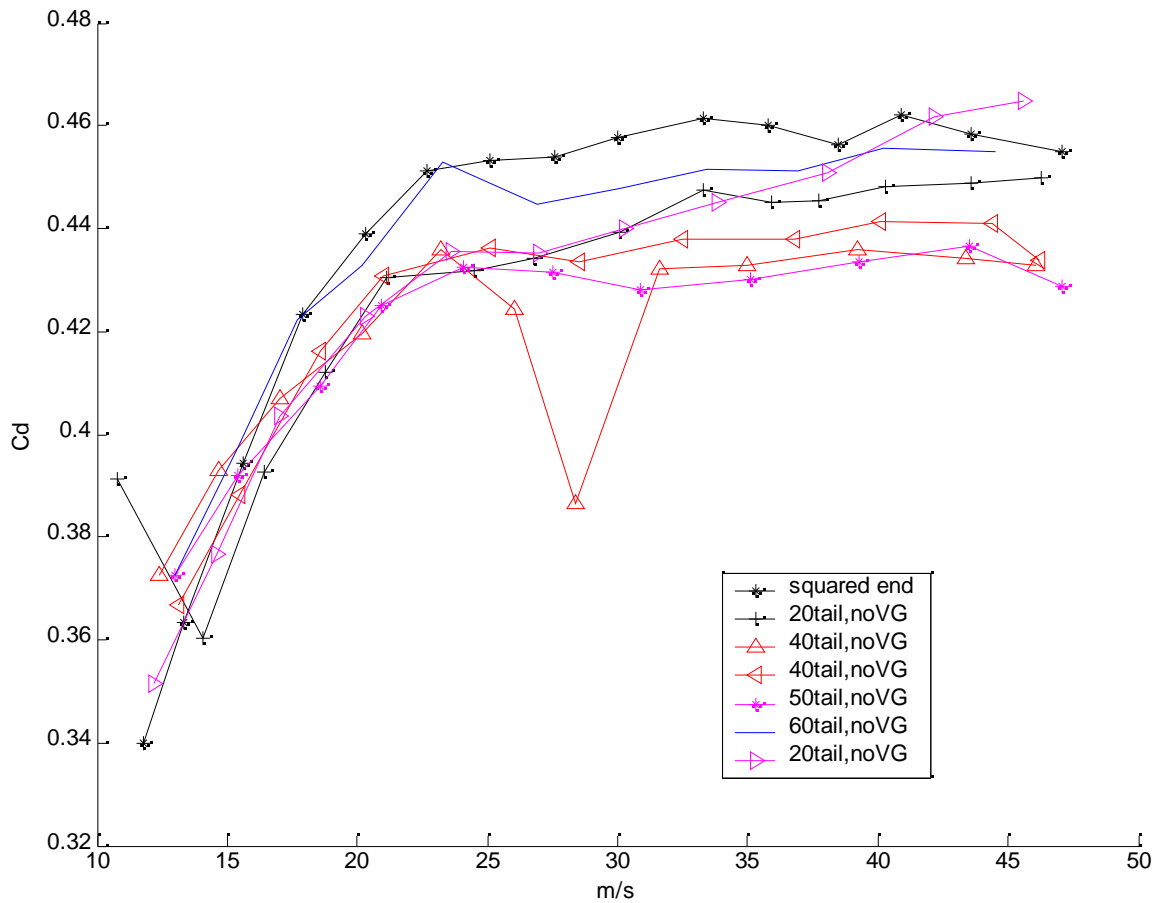
Figure 19: Drag versus airflow speed for different configurations without VG.
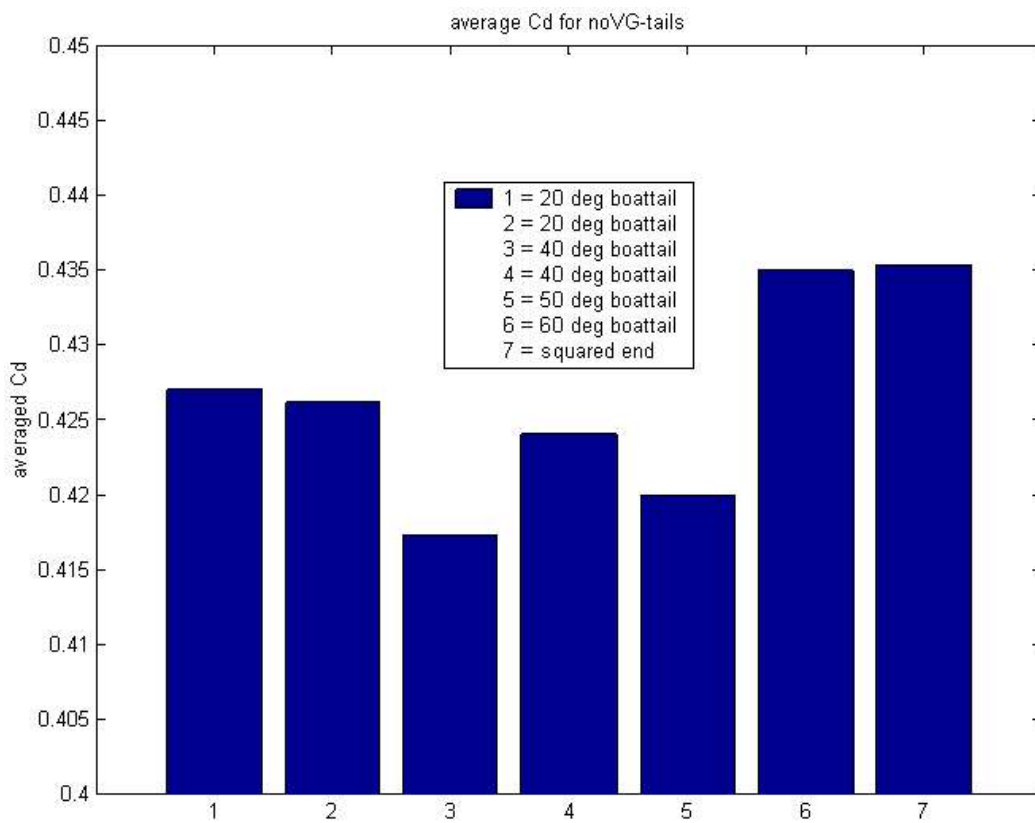
Figure 20: Drag versus degree of boat-tailing without VGs.

25

Figure 21 show that the drag varies with different location and spacing of VGs for the 40°
boat-tail. But it also shows that the lowest value of drag is received when no VGs are mounted
on the 40° boat-tail.
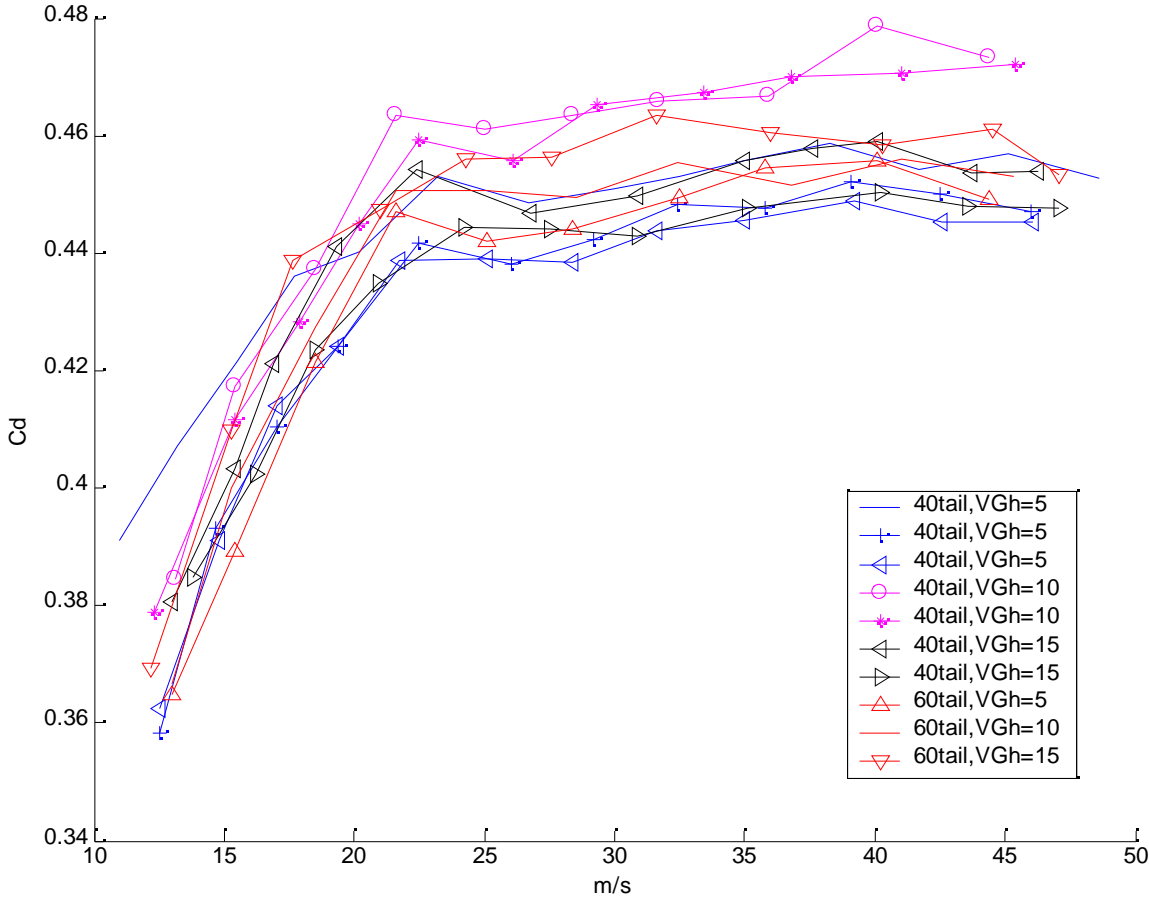
Figure 21: Drag versus airflow speed for different configurations with VG.

5.5 Third wind tunnel test series

A third series of wind tunnel tests were performed 2004-03-26 to investigate if drag could be reduced by mounting VGs in before the shoulder of the boattail. Full results of tests performed can be found in Appendix 3, a summary with the most interesting results is presented in figure 22.
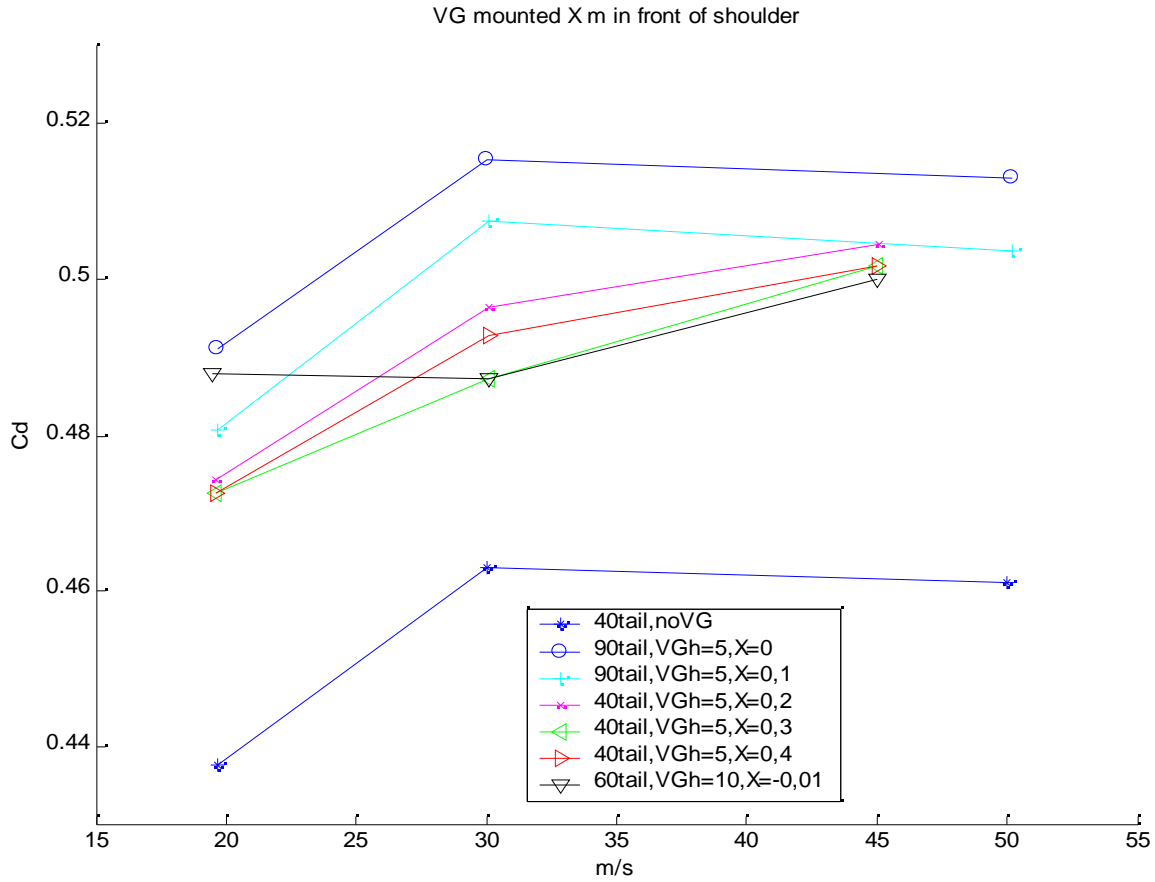
Figure 22: Summary of tests performed 2004-03-26.

Lowest drag configuration is when a boattail with no VGs is mounted.

Comparisons made with Xfoil simulations give that the windtunnel tests confirm the values recieved with Xfoil i.e. increasing C_d with increased rear angle of body.

6 Conclusions

These results indicate that it doesn't seems to be any point in mounting VGs just behind the shoulder of a diffuser as described by figure 2. The most beneficial approach in reducing bluff body drag seems to be to equip it with a 50° boat-tail.

But since equation (7) indicates that the boundary layer is approximately 17 mm thick the use of 10 mm and 15 mm height VGs could be considered as "over-achievement". More beneficial result would probably be received with the use of low-profile vortex generators as suggested by Lin [11] and this could result in a configuration that is useful in reducing drag on commercial vehicles.

The goal would be to produce a drag reduction in the area of what is received using a 20° boat-tail but without the downsides of reduced load and passenger compartment.

Based on the studies done by Torbjörn Gustavsson [12] there are several indications that the uses of low-profile VGs are beneficial for drag reduction on aeroplanes and diffusers.

Tests done so far can not be considered as conclusive but would suggest more research in the area. The results can be used as an indication where the most interesting results can be found.

In the measured results for a 40º boattail the results differ by approximately 9 %. That gives some suggestion about the accuracy of the measurements done in the Västerås facility. The results would have benefited of additional bench-mark-testing to validate that repeated tests with the same setup generate the same result.

7   References

[1] Wolf-Heinrich Hucho; Aerodynamics of Road Vehicles, ISBN 0-7680-0029-7

[2] Alfons Gilhaus; The main parameters determining the aerodynamic drag of buses, Neue Technologie, M.A.N. München, June 1981

[3] W. Calarese, W.P. Crisler and G.L. Gustafson; Afterbody Drag Reduction by Vortex Generators, Flight Dynamics Laboratory, Air Force Wright Aeronautical Laboratories, Wright_Patterson Air Force base, Ohio. AIAA-85-0354. January 14-17, 1985/ Reno, Nevada

[4] S. Klausmeyer, M. Papadakis, J. Lin; A Flow Phisics Study of Vortex Generators on a Multi-Element Airfoil, AIAA 96-0548

[5] Sven-Olof Ridder, Hans Göran Lorinder; Vehicle, especially a station vagon, having a vortex generator for producing an attached flow over the rear window, Appl. No. 113,239. Feb. 8, 1971

[6] http://raphael.mit.edu/xfoil/

[7] R H Barnard; Road Vehicle Aerodynamic Design. ISBN 0-9540734-0-1

[8] www.vortaflow.com/downloads

[9] John D. Andersson, JR; Introduction to flight, ISBN 0-07-001641-0

[10] http://aerodyn.org/WindTunnel/ttunnels.html

[11] John C. Lin; Review of research on low-profile vortex generators to control boundary-layer separation. Progress in Aerospace Sciences 38 (2002) 389-420.

[12] Torbjörn Gustavsson – Alternative approaches to rear end drag reduction

8 Appendix 1 – detailed description of the Västerås wind-tunnel facility
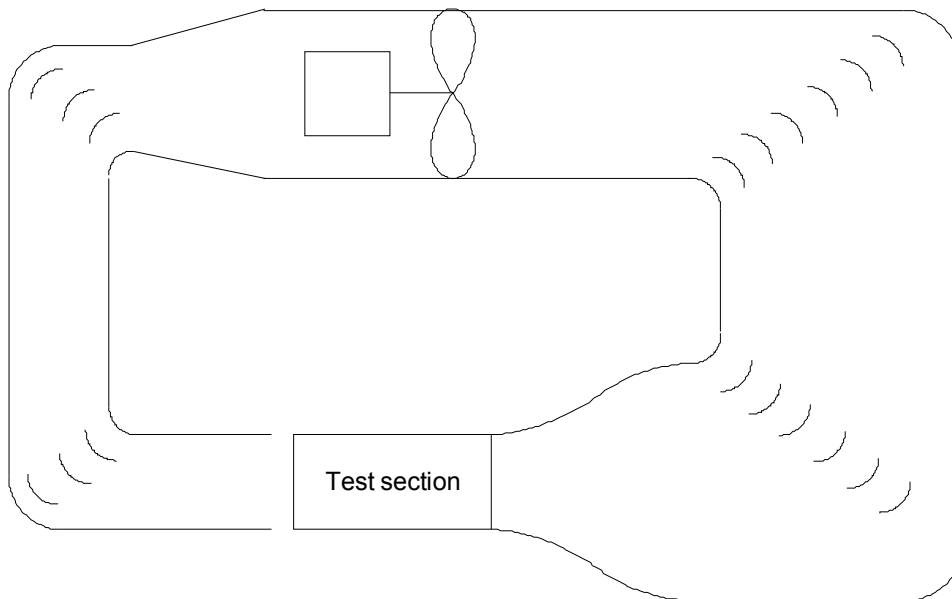
Test section:
Width: 1000 mm
Height: 750 mm
Length: 2300mm
PIAB instruments calibrated to 0.5 %
Pitottube resolution: 1 Pa
Max hastighet: 65 m/s

Rest of tunnel:
Length of contraction: 2500 mm
Diffusorns längd: honeycomb 70mm

Other parts of tunnel:
Inner height: max 2500mm
Inner width: max 3000mm
Length of section containing engine: 13m
Total length of side containing test section: 13 m
Overall total length: 40 m

Engine/ fan data:
Max: 1100 rpm
Rpm control in increments of: no steps
Length: 3000mm with contraction front and rear
Engine diameter: max 500 främre kon

Air speeds: 5 - 65 m/s

9 Appendix 2 – detailed description of wind-tunnel balance
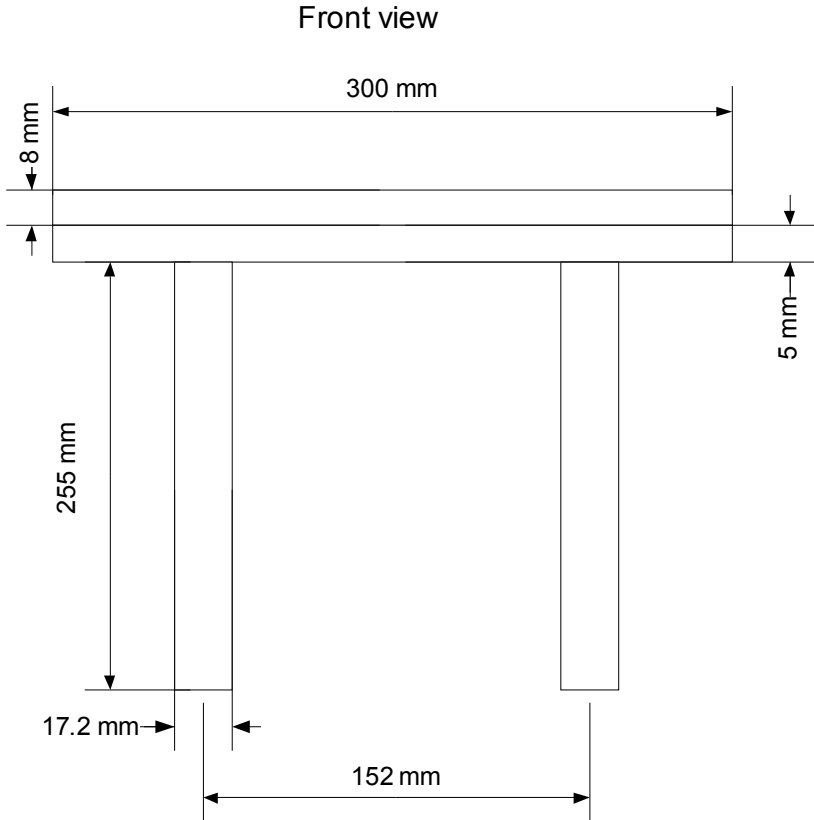
Front view

Figure 8: Front view of wind-tunnel balance.
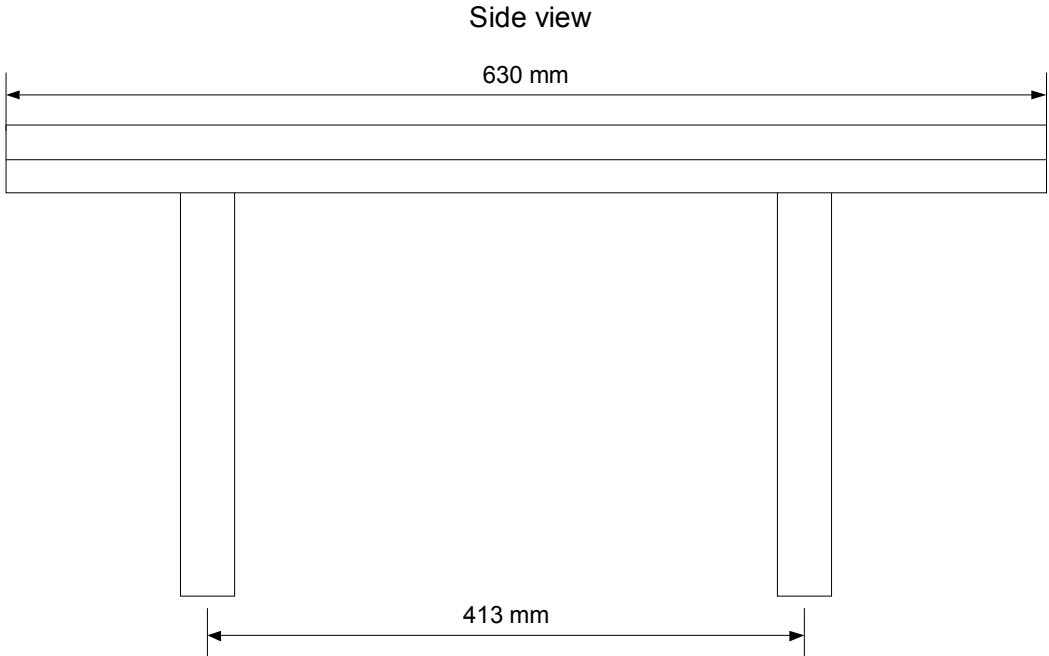
Side view

Figure 9: Side view of wind-tunnel balance.

Loadingcell: Piab
Max load: 100 N
Resolution: 0.01 N.

10 Appendix 3 – Test results of windtunnel tests 2004-03-26

Test number	Boat-tail: 20°, 40°, 60°, 90°	VG height, [mm]	VG length, [mm]	VGspacing, [mm] Front / rear edge	Co- or counter-rotating vorticies	Distance from rear edge, [m]	Cd
1	Empty channel	-	-	-	-	-	0.2839
2	20	-	-	-	-	-	0.4610
3	40	-	-	-	-	-	0.4540
4	60	-	-	-	-	-	0.4780
5	90	-	-	-	-	-	0.4744
6	40	5	5	5/10	counter	0	0.5242
7	60	"	"	"	"	"	0.5023
8	90	"	"	"	"	"	0.5065
9	40	"	"	"	"	0,1	0.5097
10	60	"	"	"	"	"	0.5097
11	90	"	"	"	"	"	0.4973
12	40	"	"	"	"	0,2	0.4918
13	60	"	"	"	"	"	0.5063
14	90	"	"	"	"	"	0.5069
15	40	"	"	"	"	0,3	0.4873
16	60	"	"	"	"	"	0.5092
17	90	"	"	"	"	"	0.5046
18	40	"	"	"	"	0,4	0.4891
19	60	"	"	"	"	"	0.5049
20	90	"	"	"	"	"	0.5057
21	40	"	"	"	"	BS	0.4918
22	60	"	"	"	"	"	0.4923
23	40	10	5	15/25	counter	0	0.5319
24	60	"	"	"	"	"	0.5200
25	90	"	"	"	"	"	0.5198
26	40	"	"	"	"	0,1	0.5221
27	60	"	"	"	"	"	0.5281
28	90	"	"	"	"	"	0.5164
29	40	"	"	"	"	0,2	0.5178
30	60	"	"	"	"	"	0.5218
31	90	"	"	"	"	"	0.5139
32	40	"	"	"	"	0,3	0.5078
33	60	"	"	"	"	"	0.5212
34	90	"	"	"	"	"	0.5150
35	40	"	"	"	"	0,4	0.5040

36	60	"	"	"	"	"	0.5159
37	90	"	"	"	"	"	0.5215
38	40	"	"	"	"	BS	0.5104
39	60	"	"	"	"	"	0.4919
40	40	15	5	20/35	counter	0	0.5307
41	60	"	"	"	"	"	0.5290
42	90	"	"	"	"	"	0.5275
43	40	"	"	"	"	0,1	0.5388
44	60	"	"	"	"	"	0.5390
45	90	"	"	"	"	"	0.5281
46	40	"	"	"	"	0,2	0.5359
47	60	"	"	"	"	"	0.5408
48	90	"	"	"	"	"	0.5319
49	40	"	"	"	"	0,3	0.5307
50	60	"	"	"	"	"	0.5352
51	90	"	"	"	"	"	0.5319
52	40	"	"	"	"	0,4	0.5227
53	60	"	"	"	"	"	0.5335
54	90	"	"	"	"	"	0.5340
55	40	"	"	"	"	BS	0.5039
56	60	"	"	"	"	"	0.4950

Table 3: Different test setups. BS = Behind Shoulder, as legislated by SNRA

noVG

VG mounted after shoulder

VG mounted just at shoulder
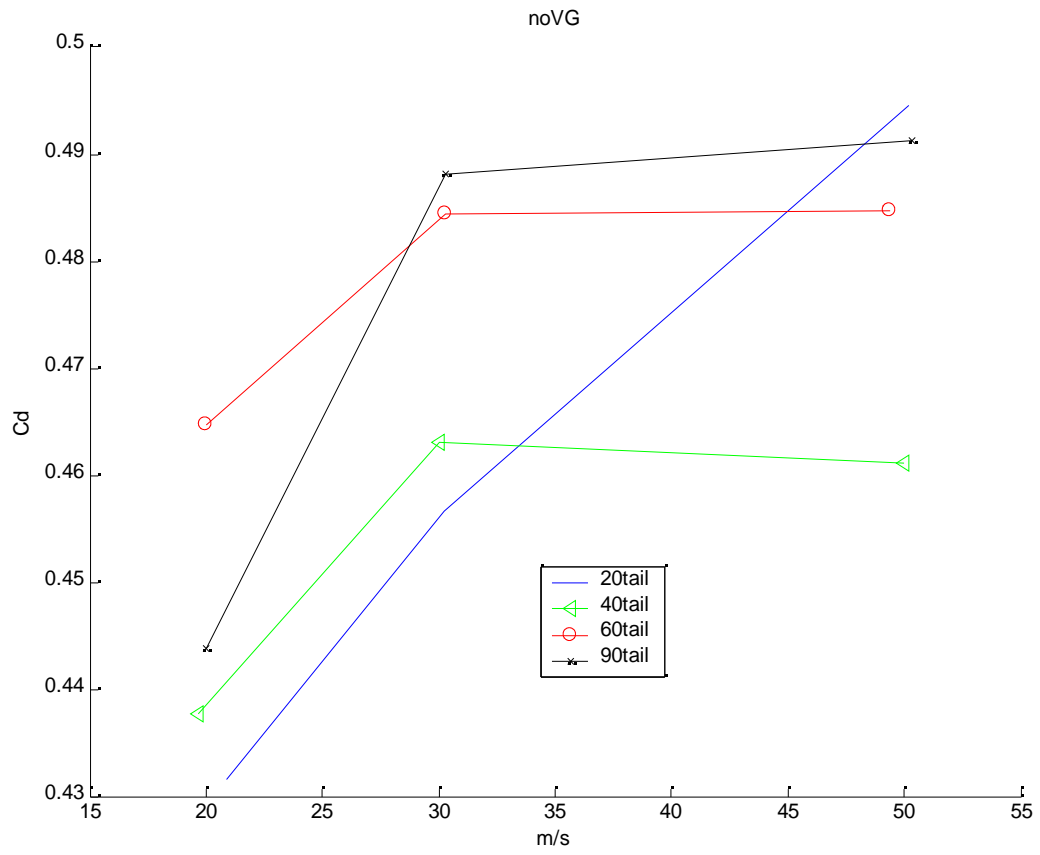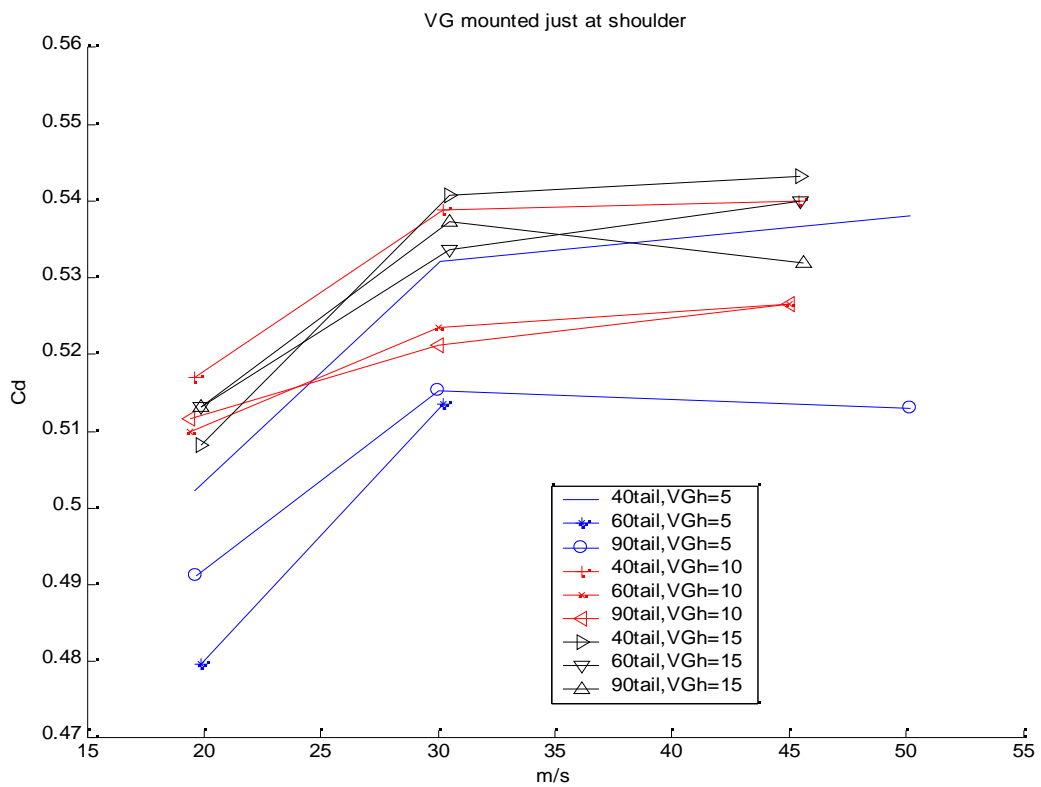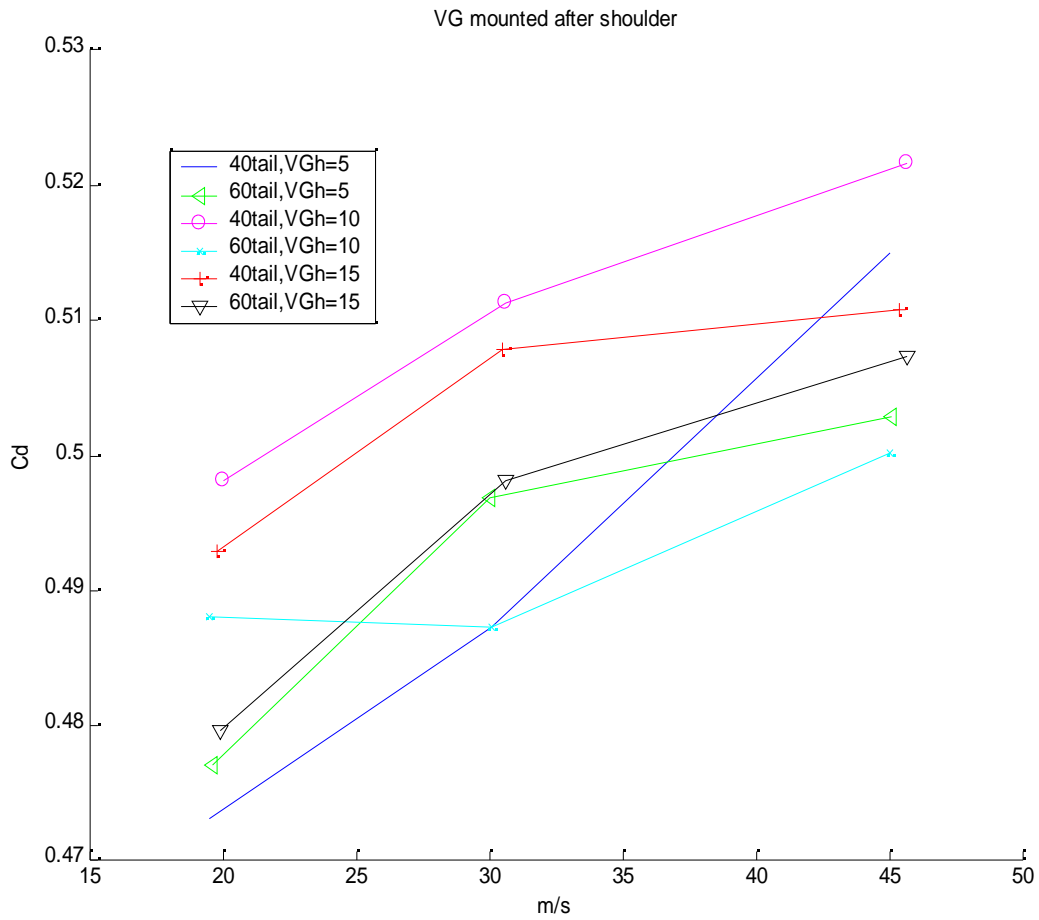
A small mistake in the measurement of 60tail give inconclusive results for that value.

VG mounted 0,1 m in front of shoulder

VG mounted 0,2 m in front of shoulder

VG mounted 0,3 m in front of shoulder

VG mounted 0,4 m in front of shoulder